
Capturing infinitely sharp discrete shock profiles with the Godunov scheme

Chalons C.¹ and Coquel F.²

¹ Université Paris 7 & Laboratoire JLL, U.M.R. 7598, Boîte courrier 187, 75252 Paris Cedex 05, France. chalons@math.jussieu.fr

² CNRS & Laboratoire JLL, U.M.R. 7598, Boîte courrier 187, 75252 Paris Cedex 05, France. coquel@ann.jussieu.fr

Summary. We show how to generate infinitely sharp discrete shock profiles with the Godunov method. This work is a first step towards the computation of nonclassical solutions associated with systems having at least one non genuinely nonlinear nor linearly degenerate characteristic field.

1 Introduction and motivations

In this paper, we consider a nonlinear hyperbolic system of N conservation laws in one space dimension :

$$\begin{cases} \partial_t \mathbf{v} + \partial_x \mathbf{f}(\mathbf{v}) = 0, \\ \mathbf{v}(x, 0) = \mathbf{v}_0(x), \end{cases} \quad (x, t) \in \mathbb{R} \times \mathbb{R}^{+*}, \quad \mathbf{v}(x, t) \in \mathbb{R}^N. \quad (1)$$

It is well-known that this problem generally does not admit smooth solutions for large times so that weak solutions in the sense of distributions are considered. Due to the presence of discontinuities, these are generally not uniquely determined by \mathbf{v}_0 and the validity of an entropy criterion is added for the admissibility of discontinuities. More precisely, (1) is supplemented with the following entropy inequality

$$\partial_t U(\mathbf{v}) + \partial_x F(\mathbf{v}) \leq 0, \quad (2)$$

to be satisfied in the sense of distributions. In (2), (U, F) is assumed to be an entropy-entropy flux pair (see [2]).

When (1) is strictly hyperbolic and admits only genuinely nonlinear (GNL) or linearly degenerate (LD) characteristic fields, existence and uniqueness of an entropy solution is proved for the Cauchy problem (1)-(2) (see for instance [1] for a review). From a numerical point of view, the celebrated Godunov method is an example of conservative and entropic numerical strategy that provides good numerical approximations. In fact, the method converges (if it

does) towards the unique entropy solution under consideration by the Lax-Wendroff theorem (see [2] for details).

The situation becomes more complicated when one characteristic field (at least) is neither GNL nor LD. In this context, admissible weak solutions of (1)-(2) are no longer unique and an additional selection criterion must be introduced for shock discontinuities. This criterion is often called *kinetic criterion* and may take various forms (see [3]). For instance, the selection of admissible shock waves of (1)-(2) can be determined by the travelling waves associated with an augmented system of the following form

$$\partial_t \mathbf{v} + \partial_x \mathbf{f}(\mathbf{v}) = \partial_x \mathcal{R}(\varepsilon \partial_x \mathbf{v}, \delta \varepsilon^2 \partial_{xx} \mathbf{v}) \quad (3)$$

which incorporates the effects of small scales like viscosity and capillarity. In (3), the rescaling parameter ε is expected to be very small, and δ represents the strength of the capillarity. This definition of admissible shock turns out to be very sensitive with respect to δ when one characteristic field fails to be either GNL or LD : two distinct values of δ generically give birth to two different families of admissible discontinuities in the limit system (1)-(2). The consequence of this sensitiveness is that the numerical approximation of the weak solutions of (1)-(2) becomes a particularly challenging issue. For instance, the Godunov method itself fails in providing good numerical approximations. The reason of this failure is that the artificial diffusion terms induced by most of the numerical methods generally disagree with the regularization operator \mathcal{R} (that is with the prescribed value of δ) and eventually corrupt the discrete shocks. By contrast, the Glimm random choice method stays free from artificial numerical diffusion and converges to the correct solution. In particular, it provides sharp discrete shock profiles.

The difficulty in approximating the solutions of such systems being related to the artificial numerical diffusion, our main purpose in this paper is to propose a numerical strategy based on the Godunov method which is free of numerical diffusion across the shock waves, in the classical framework of GNL or LD fields. From now on, we then assume that (1)-(2) is strictly hyperbolic with either GNL or LD characteristic fields. We claim that with such an algorithm providing infinitely sharp discrete shock profiles, we will be in a better position to tackle the general case in a forthcoming study.

2 The numerical approximation

Let us first introduce a time step Δt and a space step Δx that we assume to be constant for simplicity in the forthcoming developments. We set $\lambda = \frac{\Delta t}{\Delta x}$ and define the mesh interfaces $x_{j+1/2} = j\Delta x$ for $j \in \mathbb{Z}$, and the intermediate times $t^n = n\Delta t$ for $n \in \mathbb{N}$. In the sequel, \mathbf{v}_j^n denotes the approximated value at time t^n and on the cell $\mathcal{C}_j = [x_{j-1/2}, x_{j+1/2}[$ of the solution of (1)-(2). Therefore, a piecewise constant approximated solution $x \rightarrow \mathbf{v}_\lambda(x, t^n)$ at time

t^n is given by $\mathbf{v}_\lambda(x, t^n) = \mathbf{v}_j^n$ for all $x \in \mathcal{C}_j$, $j \in \mathbb{Z}$, $n \in \mathbb{N}$. When $n = 0$, we set for instance

$$\mathbf{v}_j^0 = \frac{1}{\Delta x} \int_{x_{j-1/2}}^{x_{j+1/2}} \mathbf{v}_0(x) dx, \quad \forall j \in \mathbb{Z}.$$

We follow by briefly recalling the two steps of the celebrated Godunov method.

Step 1 : Evolution in time

In this first step, one solves the following Cauchy problem

$$\begin{cases} \partial_t \mathbf{v} + \partial_x \mathbf{f}(\mathbf{v}) = 0, & x \in \mathbb{R}, \\ \mathbf{v}(x, 0) = \mathbf{v}_\lambda(x, t^n), \end{cases} \quad (4)$$

for times $t \in [0, \Delta t]$. Recall that $x \rightarrow \mathbf{v}_\lambda(x, t^n)$ is piecewise constant. Then, under the following usual CFL restriction involving the characteristic speeds $\lambda_i, i = 1, \dots, N$ of (1) :

$$\frac{\Delta t}{\Delta x} \max_{\mathbf{v}} \{|\lambda_i(\mathbf{v})|, i = 1, \dots, N\} \leq \frac{1}{2}, \quad (5)$$

for all the \mathbf{v} under consideration, the solution of (4) is known by glueing together the solutions of the Riemann problems set at each interface (see figure 1). More precisely

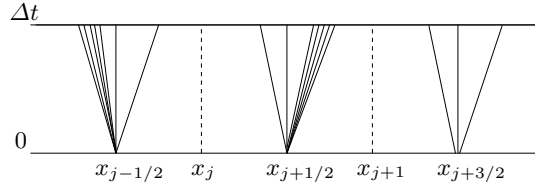


Fig. 1. An example of Riemann solutions at each interface

$$\mathbf{v}(x, t) = \mathbf{v}_r\left(\frac{x - x_{j+1/2}}{t}; \mathbf{v}_j^n, \mathbf{v}_{j+1}^n\right) \text{ for all } (x, t) \in [x_j, x_{j+1}] \times [0, \Delta t], \quad (6)$$

where $(x, t) \rightarrow \mathbf{v}_r(\frac{x}{t}; \mathbf{v}^l, \mathbf{v}^r)$ denotes the self-similar solution of the Riemann problem

$$\begin{cases} \partial_t \mathbf{v} + \partial_x \mathbf{f}(\mathbf{v}) = 0, & x \in \mathbb{R}, t \in \mathbb{R}^{+,*} \\ \mathbf{v}(x, 0) = \begin{cases} \mathbf{v}^l & \text{if } x < 0, \\ \mathbf{v}^r & \text{if } x > 0, \end{cases} \end{cases} \quad (7)$$

whatever \mathbf{v}^l and \mathbf{v}^r are in the phase space.

Step 2 : Projection

In this second step, we get back a piecewise constant approximated solution on each cell \mathcal{C}_j at time t^{n+1} by averaging the solution $x \rightarrow \mathbf{v}(x, \Delta t)$:

$$\mathbf{v}_j^{n+1} = \frac{1}{\Delta x} \int_{x_{j-1/2}}^{x_{j+1/2}} \mathbf{v}(x, \Delta t) dx, \quad j \in \mathbb{Z}. \quad (8)$$

Using Green's formula, we get the usual conservative update formula

$$\mathbf{v}_j^{n+1} = \mathbf{v}_j^n - \lambda(\mathbf{g}_{j+1/2} - \mathbf{g}_{j-1/2}) \quad \text{with} \quad \mathbf{g}_{j+1/2} = \mathbf{f}(\mathbf{v}_r(0^\pm; \mathbf{v}_j^n, \mathbf{v}_{j+1}^n)). \quad (9)$$

As already stated in the introduction, this method is shown to be entropic (by Jensen's inequality) and generally gives numerical solutions in good agreement with exact ones. However, the associated discontinuities are generally smeared at the discrete level and even if this point is natural, it is not satisfactory with respect to our objective in this paper. Actually, there exists a very particular situation for which the Godunov method does not produce smeared shock profiles, namely when considering an isolated stationary discontinuity. Indeed, if we consider a Riemann problem (7) such that \mathbf{v}^l and \mathbf{v}^r can be joined by an admissible stationary discontinuity, Godunov's method is by construction exact and then keeps sharp the discontinuity. This property is in fact the starting point in the design of our numerical strategy for obtaining sharp discrete shock (moving or not) profiles. We are going to make artificially stationary in a first step all the shocks arising in the Riemann solutions set at interfaces $x_{j+1/2}$, the dynamics being taken into account in a second step. We hope in this way to get back sharp numerical shocks provided that a relevant method is used in the second step.

Before describing our numerical strategy in details, let us first be more precise on the proposed two-step decomposition. For that, let be given \mathbf{v}_j^n and \mathbf{v}_{j+1}^n such that the corresponding Riemann solution $(x, t) \rightarrow \mathbf{v}_r(\frac{x-x_{j+1/2}}{t}; \mathbf{v}_j^n, \mathbf{v}_{j+1}^n)$ contains an admissible shock. We denote $\sigma_{j+1/2}$ its speed of propagation and $\mathbf{v}_{j+1/2}^{n-}$ and $\mathbf{v}_{j+1/2}^{n+}$ its left and right states, see figure 2.

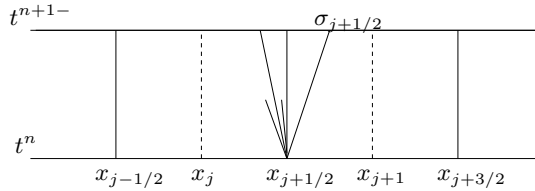


Fig. 2. An example of Riemann solution containing a shock wave

On the interval $[x_j, x_{j+1}]$, we first rewrite equivalently $\partial_t \mathbf{v} + \partial_x \mathbf{f}(\mathbf{v}) = 0$ as $\partial_t \mathbf{v} + \partial_x \mathbf{f}(\mathbf{v}) - \sigma_{j+1/2} \partial_x \mathbf{v} + \sigma_{j+1/2} \partial_x \mathbf{v} = 0$ and we then propose to solve it using a splitting strategy :

First step ($t^n \rightarrow t^{n+1-}$) This step consists in solving

$$\begin{cases} \partial_t \mathbf{v} + \partial_x \mathbf{f}(\mathbf{v}) - \sigma_{j+1/2} \partial_x \mathbf{v} = 0 \\ \mathbf{v}(x, 0) = \begin{cases} \mathbf{v}_j^n & \text{if } x < 0, \\ \mathbf{v}_{j+1}^n & \text{if } x > 0, \end{cases} \end{cases} \quad (10)$$

still supplemented with the entropy inequality (2). It is clear at this stage that the Riemann solution $(x, t) \rightarrow \tilde{\mathbf{v}}_{\mathbf{r}}(\frac{x-x_{j+1/2}}{t}; \mathbf{v}_j^n, \mathbf{v}_{j+1}^n)$ of (10) is obtained by simply shifting $(x, t) \rightarrow \mathbf{v}_{\mathbf{r}}(\frac{x-x_{j+1/2}}{t}; \mathbf{v}_j^n, \mathbf{v}_{j+1}^n)$ so as to get

$$\tilde{\mathbf{v}}_{\mathbf{r}}(\frac{x-x_{j+1/2}}{t}; \mathbf{v}_j^n, \mathbf{v}_{j+1}^n) = \mathbf{v}_{\mathbf{r}}(\frac{x-x_{j+1/2} + \sigma_{j+1/2}t}{t}; \mathbf{v}_j^n, \mathbf{v}_{j+1}^n),$$

see figure 3. Observe that the discontinuity associated with the shock wave

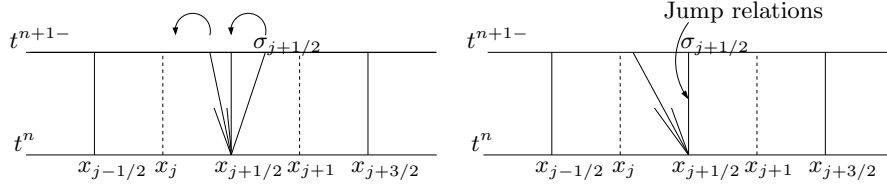


Fig. 3. Illustration of the rotation on a Riemann solution containing a shock wave

under consideration is now located along the $x = x_{j+1/2}$ -axis. In other words, the shock has been made artificially stationary. When using the Godunov method in this first step, the generated discrete shock profiles are thus expected to be sharp.

Second step ($t^{n+1-} \rightarrow t^{n+1}$) This step takes into account the dynamics of the shock wave left stationary in the first step. It amounts to solve the following transport equation :

$$\partial_t \mathbf{v} + \sigma_{j+1/2} \partial_x \mathbf{v} = 0, \quad (11)$$

see figure 4. The solution obtained at the end of the first step will serve as a natural initial data for (11). In order to keep sharp the numerical profiles that are expected to be generated by the first step, we will make use of a random sampling strategy.

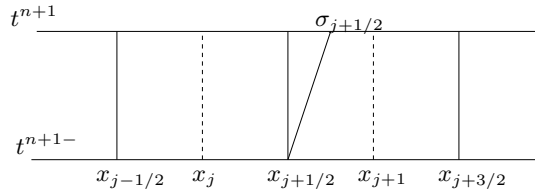


Fig. 4. Accounts for the dynamics of the shock wave in the splitting strategy

Let us now describe the full strategy with details.

First step ($t^n \rightarrow t^{n+1-}$): *the Godunov method*

At each interface $x_{j+1/2}$, let us define $\sigma_{j+1/2}$ and $\mathbf{v}_{j+1/2}^{n\pm}$ as follows :

- if there is at least one shock wave in the Riemann solution $(x, t) \rightarrow$

$\mathbf{v}_r(\frac{x-x_{j+1/2}}{t}; \mathbf{v}_j^n, \mathbf{v}_{j+1}^n)$, then $\sigma_{j+1/2}$, $\mathbf{v}_{j+1/2}^{n-}$ and $\mathbf{v}_{j+1/2}^{n+}$ are respectively the speed of propagation and the corresponding left and right states of the shock with the larger amplitude for a given norm,

- otherwise, we set $\sigma_{j+1/2} = 0$ and $\mathbf{v}_{j+1/2}^{n\pm} = \mathbf{v}_r(0^\pm; \mathbf{v}_j^n, \mathbf{v}_{j+1}^n)$.

Then, under the CFL restriction

$$\frac{\Delta t}{\Delta x} \max_{\mathbf{v}} \{|\lambda_i(\mathbf{v})|, i = 1, \dots, N\} \leq \frac{1}{4}, \quad (12)$$

for all the \mathbf{v} under consideration, which is more restrictive than (5) due to the shift, we can define the function $(x, t) \rightarrow \tilde{\mathbf{v}}(x, t)$ for all $x \in \mathbb{R}$ and $t \in [0, \Delta t]$ as the juxtaposition of the Riemann solutions $(x, t) \rightarrow \tilde{\mathbf{v}}_r(\frac{x-x_{j+1/2}}{t}; \mathbf{v}_j^n, \mathbf{v}_{j+1}^n)$ defined on each interval $[x_j, x_{j+1}]$. By averaging on each cell \mathcal{C}_j this solution at time Δt as in the usual Godunov method, we arrive at the following definition :

$$\mathbf{v}_j^{n+1-} = \frac{1}{\Delta x} \int_{x_{j-1/2}}^{x_{j+1/2}} \tilde{\mathbf{v}}(x, \Delta t) dx, \quad j \in \mathbb{Z}.$$

Invoking again the Green formula, a straightforward calculation leads now to

$$\mathbf{v}_j^{n+1-} = \mathbf{v}_j^n - \lambda(\tilde{\mathbf{g}}_{j+1/2} - \tilde{\mathbf{g}}_{j-1/2}) - \lambda(\sigma_{j+1/2} - \sigma_{j-1/2}) \mathbf{v}_j^n$$

with $\tilde{\mathbf{g}}_{j+1/2} = \mathbf{f}(\mathbf{v}_{j+1/2}^{n\pm}) - \sigma_{j+1/2} \mathbf{v}_{j+1/2}^{n\pm}$. Note that $\mathbf{f}(\mathbf{v}_{j+1/2}^{n-}) - \sigma_{j+1/2} \mathbf{v}_{j+1/2}^{n-} = \mathbf{f}(\mathbf{v}_{j+1/2}^{n+}) - \sigma_{j+1/2} \mathbf{v}_{j+1/2}^{n+}$ by the jump relations across the shock wave, while if $\sigma_{j+1/2} = 0$ these numerical fluxes coincide with those of the usual Godunov method.

Second step ($t^{n+1-} \rightarrow t^{n+1}$) : a sampling strategy

In this step, we solve locally at each interface $x_{j+1/2}$ the transport equation (11) whose speed is $\sigma_{j+1/2}$. As an initial data, we consider the piecewise constant solution provided at time t^{n+1-} by the first step. In order to define the new approximation \mathbf{v}_j^{n+1} at time $t^{n+1} = t^n + \Delta t$, we then propose to pick up randomly on the cell \mathcal{C}_j a value at time Δt in the juxtaposition of the solutions of the transport equations. This choice is natural in order to avoid the appearance of new values in the shock profiles generated by the first step. More precisely, given a well distributed random sequence (a_n) in $(0, 1)$, it amounts to set :

$$\mathbf{v}_j^{n+1} = \begin{cases} \mathbf{v}_{j-1}^{n+1-} & \text{if } a_{n+1} \in [0, \lambda\sigma_{j-1/2}^+[, \\ \mathbf{v}_j^{n+1-} & \text{if } a_{n+1} \in [\lambda\sigma_{j-1/2}^+, 1 + \lambda\sigma_{j+1/2}^-[, \\ \mathbf{v}_{j+1}^{n+1-} & \text{if } a_{n+1} \in [1 + \lambda\sigma_{j+1/2}^-, 1[, \end{cases} \quad (13)$$

with $\sigma_{j+1/2}^+ = \max(\sigma_{j+1/2}, 0)$ and $\sigma_{j+1/2}^- = \min(\sigma_{j+1/2}, 0)$. See also figure 5. In practice, we will use the celebrated van der Corput random sequence.

3 Numerical experiments

In this section, we give some numerical evidences to illustrate the relevance of our strategy. To that purpose, we first consider without restriction the

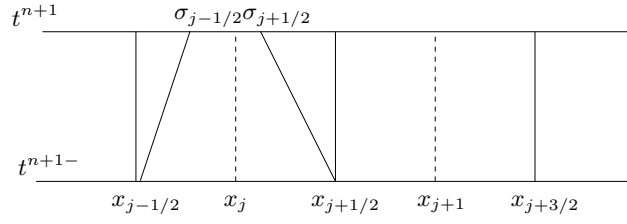


Fig. 5. Illustration of the solutions arising in the second step

p -system in Lagrangian coordinates :

$$\begin{cases} \partial_t \tau - \partial_x u = 0 & (x, t) \in \mathbb{R} \times \mathbb{R}^{+*}, \\ \partial_t u + \partial_x p(\tau) = 0, \end{cases}$$

where $\tau > 0$ is the inverse of a density, u is the velocity and $p > 0$ is the pressure of the fluid. We choose for instance $p(\tau) = \frac{1}{\tau^2}$ so that the system is strictly hyperbolic with characteristic speeds $\lambda_2 = -\lambda_1 = \sqrt{-p'(\tau)}$. We consider two Riemann problems (7) associated with $\mathbf{v}^l = (0.4, 0)$, $\mathbf{v}^r = (1, 0)$ (test 1) and $\mathbf{v}^l = (0.8, 0)$, $\mathbf{v}^r = (1, -1)$ (test 2) leading to solutions respectively made of a rarefaction wave followed by a 2-shock, and a 1-shock followed by a 2-shock. The covolumes τ are shown on figure 6. We observe that our strategy provides a very good approximation with in addition infinitely sharp discrete shock profiles. We follow by considering the system of gaz dynamics

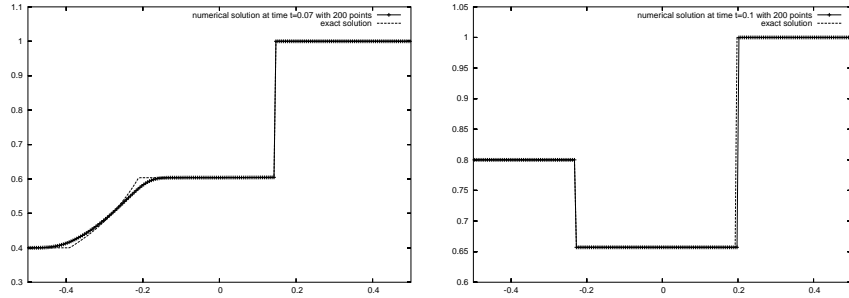


Fig. 6. τ : test 1 (Left) and test 2 (Right)

in Lagrangian coordinates

$$\begin{cases} \partial_t \tau - \partial_x u = 0 & (x, t) \in \mathbb{R} \times \mathbb{R}^{+*}, \\ \partial_t u + \partial_x p = 0, \\ \partial_t E + \partial_x p u = 0, \end{cases}$$

where $E = \frac{1}{2}u^2 + \frac{p\tau}{\gamma-1}$, $\gamma = 2$ is the total energy. This system is strictly hyperbolic with characteristic speeds $\lambda_2 = 0$ and $\lambda_3 = -\lambda_1 = \sqrt{\gamma \frac{E}{\tau}}$. We consider

two Riemann problems (7) associated with $\mathbf{v}^l = (0.5, 2, 2.625)$, $\mathbf{v}^r = (2, 1, 1)$ (test 3) and $\mathbf{v}^l = (0.2, 1, 0.7)$, $\mathbf{v}^r = (0.176, 0.875, 0.67)$ (test 4) leading to solutions respectively made of a contact discontinuity followed by a 3-shock, and a 1-shock followed by a contact discontinuity and a rarefaction wave. Again, we observe on figure 7 plotting the covolumes that our method generates infinitely sharp discrete shock profiles. With these two test cases, we also show that making stationary a shock wave in a system that already contains a stationary discontinuity (here a contact discontinuity) does not rise difficulties. In order to further validate the method, it is important to notice that when

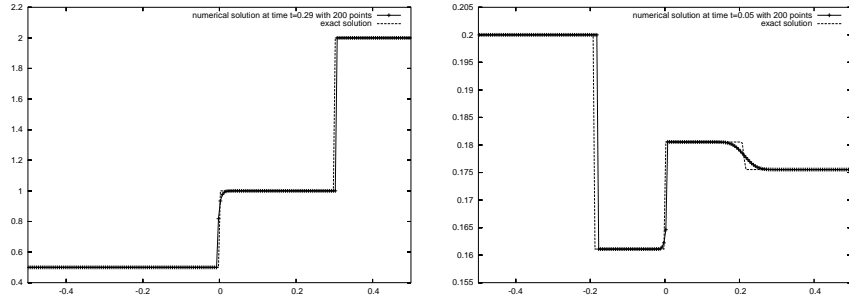


Fig. 7. τ : test 3 (Left) and test 4 (Right)

the Riemann initial data consists of two states that can be joined by an admissible shock, the proposed method simply reduces to the Glimm scheme and then converges to the expected solutions with an infinitely sharp shock profile.

As a conclusion, let us mention that it is actually possible to get rid of the exact Riemann solver used in our method while still keeping on generating infinitely sharp discrete shock profiles. Our approach is based on approximate Riemann solvers and will be describe in a longer paper. We will eventually apply the strategy for the computation of nonclassical solutions associated with non GNL nor LD fields, which is the very motivation of this study.

References

1. Bressan, A.: The semigroup approach to systems of conservation laws. *Mat. Contemp.*, **10**, 21–74 (1996)
2. Godlewsky, E., Raviart, P.-A., Numerical approximation of hyperbolic systems of conservation laws. Springer (1995)
3. LeFloch, P.-G, Hyperbolic systems of conservation laws: the theory of classical and nonclassical shock waves. Birkhäuser (2002)